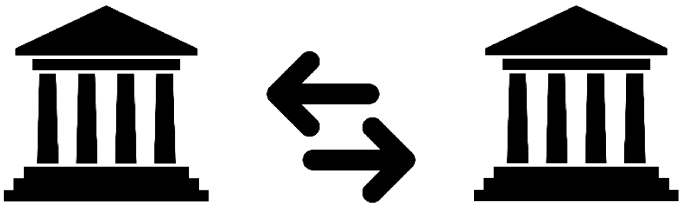

This PDF has been sent from one of the University of Delaware's partner libraries through Interlibrary Loan. It will be in your account for **30 days**. After 30 days, the PDF will be permanently deleted.

If you received the wrong item, or if there are any other problems with the PDF (such as missing pages or unclear images), **please contact the Interlibrary Loan Office**. We will ask the supplier for a corrected copy.

Interlibrary Loan Office
AskILL@udel.libanswers.com

NOTICE: WARNING CONCERNING COPYRIGHT RESTRICTIONS

The copyright law of the United States (Title 17, United States Code) governs the making of photocopies or other reproductions of copyrighted material.

Under certain conditions specified in the law, libraries and archives are authorized to furnish a photocopy or other reproduction. One of these specified conditions is that the photocopy or reproduction is not to be "used for any purpose other than private study, scholarship, or research." If a user makes a request for, or later uses, a photocopy or reproduction in excess of "fair use," that user may be liable for copyright infringement.

This institution reserves the right to refuse to accept a copying order if, in its judgment, fulfillment of the order would involve violation of copyright law.

Articles received through Interlibrary Loan may not be redistributed.

UNIVERSITY OF DELAWARE
LIBRARY, MUSEUMS & PRESS

Journal of Environmental Chemical Engineering 8 (2020) 104139

Contents lists available at ScienceDirect

Journal of Environmental Chemical Engineering

journal homepage: www.elsevier.com/locate/jece

Fe-Cu bimetallic catalyst for the degradation of hazardous organic chemicals exemplified by methylene blue in Fenton-like reaction

Thanh Binh Nguyen[a], Cheng-Di Dong[a,*], C.P. Huang[b], Chiu-Wen Chen[a], Shu-Ling Hsieh[c], Shuchen Hsieh[d,*]

[a] Department of Marine Environmental Engineering, National Kaohsiung University of Science and Technology, Kaohsiung City, 81157, Taiwan
[b] Department of Civil and Environmental Engineering, University of Delaware, Newark, 19716, DE, USA
[c] Department of Seafood Science, National Kaohsiung University of Science and Technology, Kaohsiung City, 81157, Taiwan
[d] Department of Chemistry, National Sun Yat-sen University, Kaohsiung City, 80424, Taiwan

ARTICLE INFO

Editor: Teik Thye Lim

Keywords:
Fe-Cu bimetallic
Nanoparticles
H_2O_2 activation
Methylene blue (MB)

ABSTRACT

Fe-Cu bimetallic oxide, a Fenton-like catalyst, was synthesized by a facile co-precipitation method. The physicochemical characteristics of as-synthesized Fe-Cu bimetallic composites with different Cu mass loadings were characterized. The Fe-Cu-080 composite, having suitable amount of Cu, could effectively control the size of bimetallic particles, with uniform distribution in nano range, exhibited a higher activity and stability in methylene blue (MB) mineralization. Fe-Cu-080/H_2O_2 system could work in a wide range pH with high efficiency in MB removal and low metal leaching concentration. Electron paramagnetic resonance (EPR) and fluorescence (FL) results proved that the $OH^{\cdot}$ radicals generated in Fe-Cu composite/H_2O_2 system were involved in the degradation of methylene blue (MB). The Fe-Cu-080 catalyst could be easily separation from the aqueous solution by simple external magnetic field. Fe-Cu-080 was not cytotoxic and could greatly reduce the copper toxicity. The combination of Cu-Fe in bimetallic structure was proved to be an attractive alternative method to improve the efficiency of heterogeneous Fenton-like system exemplified by the removal of organic pollutants from wastewater.

1. Introduction

Water pollution has become one of the most severe environmental problems in the world due to rapid industrial development. The potential contamination from hazardous organic chemicals to ecosystem and drinking water system have imposed adverse effects on the aquatic life and human health. Accordingly, effective processes for the removal of organic pollutant from water has attracted considerable attention. Fenton process, a typical advanced oxidation process (AOP), has received wide spread consideration for efficient removal of various organic contaminants from wastewaters [1,2]. Solid catalysts, containing $\equiv Fe^{2+}$ and $\equiv Fe^{3+}$, are able to catalyze the decomposition of H_2O_2 with the production of highly reactive $OH^{\cdot}$ radical as to destroy organic contaminants efficiently by heterogeneous Fenton reaction (Fenton-like) [3]. Fenton-like process can significantly minimize the major disadvantage of conventional homogeneous Fenton reaction such as high iron dosage, which requires additional management cost for iron-sludge [4,5].

Magnetite nanoparticles (Fe_3O_4 NPs) is a promising Fenton-like catalyst for the treatment of contaminated wastewater owing to rapid reaction and low-cost [6,7]. Moreover, Fe_3O_4 NPs can be easily separated from the reaction system after use in magnetic field, which is crucial to efficient solid-liquid separation. However, commercial Fe_3O_4 usually exhibits relatively slow reactivity at high pH [8] or do not response to energy sources such as UV [9], ultrasound [10], or microwave [11] efficiently. Therefore, alternatives for the development of efficient and stable catalysts based on magnetite are urgently needed.

Copper, a transition metal that behaves like a Fenton reagent has attracted great attention. Cu-based catalysts exhibited high reactivity toward H_2O_2 over a wide pH range [12]. Bimetallic catalysts have shown better catalytic performance than their monometallic counterparts in a wide range of heterogeneously catalyzed reaction [13]. Incorporating copper into iron containing solid matrix to fabricate bimetallic catalyst can synergistically accelerate the interfacial electron transfer and production of reactive radicals from H_2O_2 decomposition in Fenton-like reaction. It is hypothesized that copper can enhance the catalytic activity of Fe_3O_4, and that the Fe-Cu composite may be capable of carrying out redox reactions in the presence of H_2O_2.

* Corresponding authors.
E-mail addresses: cddong@nkust.edu.tw (C.-D. Dong), shsieh@faculty.nsysu.edu.tw (S. Hsieh).

https://doi.org/10.1016/j.jece.2020.104139
Received 30 March 2020; Received in revised form 21 May 2020; Accepted 2 June 2020
Available online 06 June 2020
2213-3437/ © 2020 Elsevier Ltd. All rights reserved.

Herein, the magnetic Fe-Cu bimetallic composite was prepared using a simple precipitation method. A series of Fe-Cu bimetallic composites with different Cu content were prepared. The material properties were characterized to verify the successful synthesis of the targeted bimetallic composite. Dyes from the textile industry is the major source of water pollution, besides having possible harmful effects to human health and ecological systems. In this study, methylene blue (MB), a commonly used organic dye in textile industry, was used as a model compound to evaluate the catalytic activity of the prepared materials through oxidative degradation in a Fenton-like system. Fluorescence (FL) and electronic paramagnetic resonance (EPR) were employed to identify the major reactive species in the system. Moreover, the reusability and the magnetic separation of the Fe-Cu composite were investigated. Last, the reaction mechanism was also proposed.

2. Materials and methods

2.1. Reagents

Iron (III) chloride hexahydrate ($FeCl_3.6H_2O$, ≥ 98 %), Iron (II) chloride tetrahydrate ($FeCl_2.4H_2O$, ≥ 99 %), Copper (II) chloride dehydrate ($CuCl_2.2H_2O$, 99 %), and hydrogen peroxide (H_2O_2, 35 %) were purchased from Showa Chemical Industry Co. (Japan). Sodium hydroxide (NaOH, ≥99 %) and hydrochloric acid (HCl, 37 %) were purchased from J.T. Baker (USA). Terephthalic acid ($C_8H_6O_4$, ≥ 98 %) was purchased from Sigma-Aldrich (USA). Methylene blue (MB) ($C_{16}H_{18}ClN_3S$, 99 %) was purchased from Kojima Chemicals Co. (Japan). All the chemicals were used as received without further purification.

2.2. Synthesis of Fe-Cu bimetallic catalysts

The Fe-Cu bimetallic composites were prepared by co-precipitation. In a typical procedure, 10 mL of 1 M $FeCl_3.6H_2O$ was mixed with 10 mL of 0.5 M $FeCl_2.4H_2O$ in a beaker. Then x mL (x = 0.16, 0.64, 2.56, 6.4) of 0.125 M $CuCl_2.2H_2O$ was added to the above solution under stirring for 30 min at 60 °C. 20 mL of 10 M NaOH solution was then injected dropwise into the above solution. The mixed solution was immediately transferred to a 100 mL Teflon-lined stainless steel autoclave, which was heated and maintained at 200 °C for 12 h. After cooling down to room temperature, the solid precipitates were collected by filtration, washed thoroughly with deionized water until neutral supernatant pH, and finally dried in a vacuum oven at 70 °C overnight. The bimetallic catalysts were labelled as Fe-Cu-x (x = 0.02, 0.08, 0.32 and 0.8 milimolar), where x was the molar value of Cu. Monometallic catalysts also were prepared using the same procedure for purpose of comparison.

2.3. Experimental procedure

A series of experiments were carried out to study the catalytic activity of the composites exemplified by the degradation of MB in aqueous solution. In any typical experiment, 50 mg of catalyst was added to 100 mL of mixed solution of 5 mg L^{-1} MB and 5% H_2O_2 at pH-7. The pH was adjusted with HCl 0.1 M and NaOH 0.1 M. At the given reaction time interval, the catalysts were separated using an external magnetic field, then 1 mL of supernatant was collected for analysis of MB concentration. The residual concentration of MB was determined using a UV–vis spectrometer (Hitachi U3900) at an absorption wavelength of 660 nm. Besides, mineralization of MB was evaluated in terms of total organic carbon (TOC) analyzed through a Lotix TOC Combustion Analyzer (Teledyne Tekmar, USA) equipped with a new Non-Dispersive Infrared (NDIR) detection. In addition, stability test was also conducted by performing MB degradation under the same experimental conditions for consecutive cycles. After each cycle, the material was separated by external magnet, thoroughly washed with ethanol and DI water, dried in vacuum oven, and then reused for the next cycle. Inductively couple plasma mass spectrometry (ICP-MS) (Agilent 7500a, Santa Clara, CA USA) was used to determine the amount of leached metal in the solution.

The measurement of $OH^{\cdot}$ radicals were performed for the Fenton reaction by means of terephthalic acid (TPA) fluorescence probe. Experimental procedures were similar to the measurement of Fenton reaction except that the MB aqueous solution was replaced by an aqueous solution containing 4 mM of TPA and 0.01 M NaOH. Fluoresence spectra of highly fluorescent product was measured by a Hitachi F-7000 fluorescence spectrometer at an emission wavelength of 426 nm with an excitation wavelength of 312 nm.

2.4. Surface characterization

The surface morphology of the synthesized materials was characterized by field emission scanning electron microscope (SEM, Hitachi SU8010) with an acceleration electron voltage of 15 kV. All samples were Pt-coated using Ion Sputter ε-1030 (Hitachi, Tokyo) to increase the conductivity. High-resolution transmission electron microscopy (HRTEM) was performed using JEM-2010 F (JEOL, Japan). X-ray diffraction (XRD) patterns were recorded *via* a Bruker D8 Advance X-ray diffractometer (Bruker, USA) with Ni-filtered Cu Kα radiation (λ = 1.5406 Å) operated at a generator voltage of 40 kV and an emission current of 40 mA.

The thermal stability of all samples was carried out using the thermogravimetric analyzer (TGA) (Mettler Toledo TGA/DSC 3+ STAR) in the temperature range of 30–1000 °C and heating rate of 10 °C min^{-1} under N_2 atmosphere (40 mL min^{-1}). Raman spectra were collected using a Bruker Senterra micro-Raman spectrometer equipped with a laser power of 5 W operated at a wavelength of 532 nm. Fourier transform infrared (FTIR) spectra were performed using a Thermo Nicolet iS10 spectrometer at a resolution of 2 cm^{-1} with KBr method. Electron paramagnetic resonance (EPR) spectra were recorded on EPR spectrometer (Bruker, EMX-10) working at X-band frequency of 9.49–9.88 GHz with a power of 8.02 mW. Zeta potential was measured by Zetasizer Nano ZS (Malvern) at 25 °C. The magnetic properties of the prepared catalysts were conducted by a SQUID-Quantum Design MPMS2 vibration sample magnetometer (VSM) at room temperature.

2.5. Cell toxicity tests

NRK-52E cells (normal rat kidney proximal tubule epithelial cell) were maintained with DMEM containing 10 % fetal bovine serum and 1% penicillin/streptomycin at 37 °C in a humidified atmosphere containing 5% CO_2. Cell viability was evaluated using the MTT (3-(4,5-dimethyl thiazolyl-2)-2,5-diphenyltetrazolium bromide) tetrazolium reduction assay as described by Debizot and Lang [14]. NRK-52E cells were incubated in 3-cm plates (1 × 106 cells) for 24 h. Then cells were treated by Fe-Cu 0.8 NPs, Fe_3O_4 NPs, and CuO NPs with different concentrations (25, 50, 100, 250 and 500 μg/mL) for 24 h. Cells were further incubated with MTT (0.1 mg mL^{-1}) for 3 h at 37 °C. And the optical density (OD) was measured at 570 nm. The cell viability is expressed as a percentage of the viability of the control culture.

3. Results and discussion

3.1. Characterization of Fe-Cu composite

The morphology and structure of the prepared Fe-Cu-x bimetallic particles with different Cu mass loading were observed by SEM and TEM (Fig. 1). The bimetallic Fe-Cu particles were generally spherical with some degree of aggregation. These features can be attributed to the static magnetism and surface force between copper and iron oxide. Particularly, when the theoretical Cu mass loading was increased, the particle size gradually decreased from 65 ± 5 nm (Fe-Cu-002) to

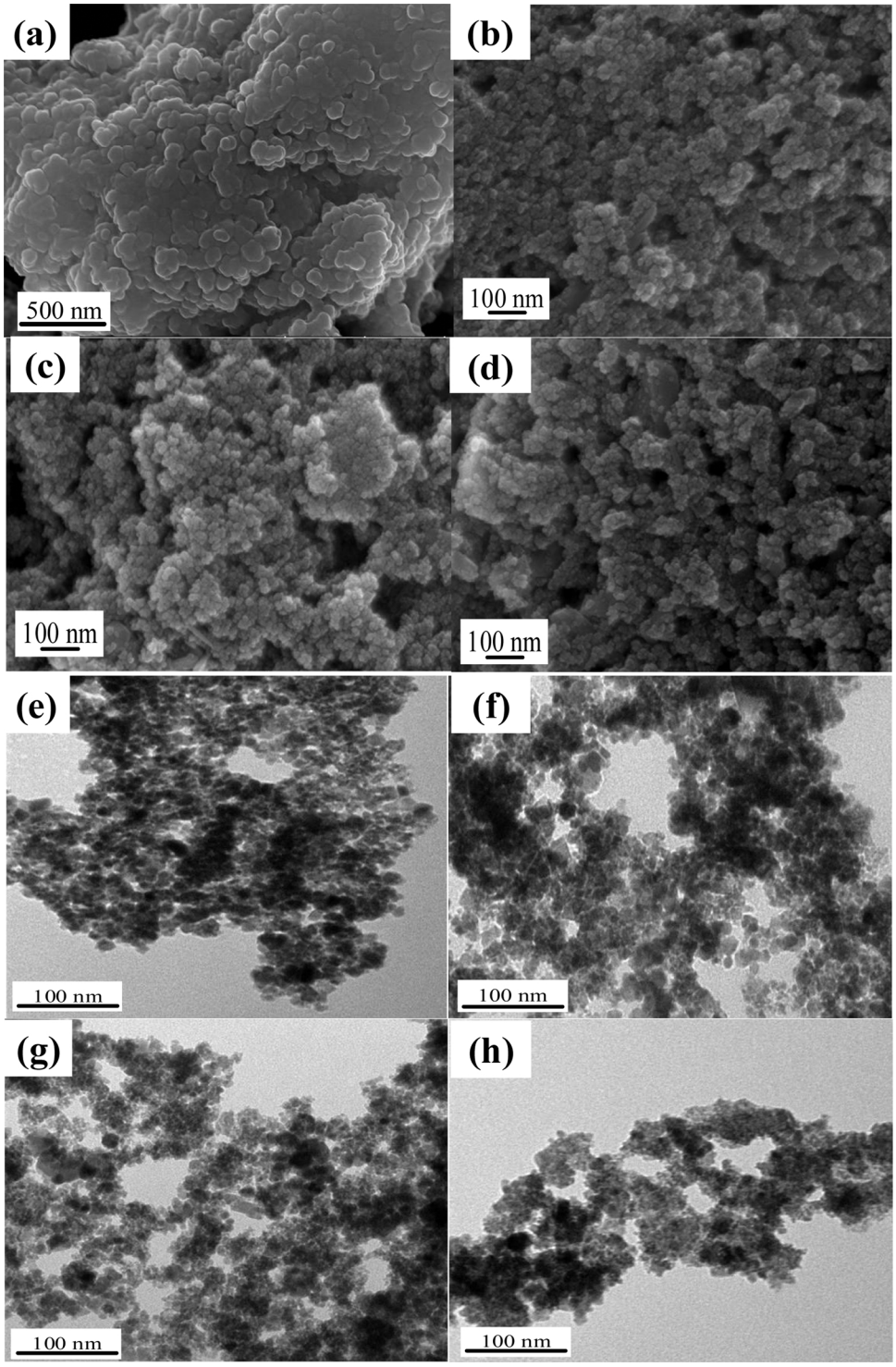

Fig. 1. SEM and TEM images of (a, e) Fe-Cu-0.02, (b, f) Fe-Cu-008, (c, g) Fe-Cu-032 and (d, h) Fe-Cu-080.

53 ± 4 nm (Fe-Cu-008), 34 ± 2 nm (Fe-Cu-032), and 12 ± 6 nm (Fe-Cu-080). The decrease in particle size after the addition of a second metal in this studies was in the same trend as that previously reported [15]. The results suggested that the loading level of Cu controlled the size distribution of bimetallic particles, especially uniform in the nano range. The presence of nano-sized metallic particles increased the active sites and improved the catalytic effectiveness.

Fig. 2**a** shows the diffraction peaks of 2θ at 30.49°, 35.95°, 43.22°, 57.22°, and 63° corresponded to [111], [311], [222], [400], [511], and [440] planes of Fe_3O_4 (JCPDS#19 − 629), clearly indicated the presence of the cubic phase of Fe_3O_4 NPs in all Fe-Cu composites. No notable XRD peaks of Cu were observed in Fe-Cu-002, 008, and 032 due to low Cu concentration [16]. XRD peaks of 2θ at 33.47°, 36.17° and 59.13° corresponded to [110], [002], and [202] planes of CuO (JCPDS#48-1548) were observed in the Fe-Cu-080 nanocomposite. The average crystallite size (dhkl) of Fe-Cu composite was calculated by using Scherrer's equation with respect to the predominant peak along the (311) direction. The crystal size was 64.17, 53.21, 34.16 and 11.74 nm for Fe-Cu-002, Fe-Cu-008, Fe-Cu-032 and Fe-Cu-080, respectively, which was in good agreement with that of TEM observation.

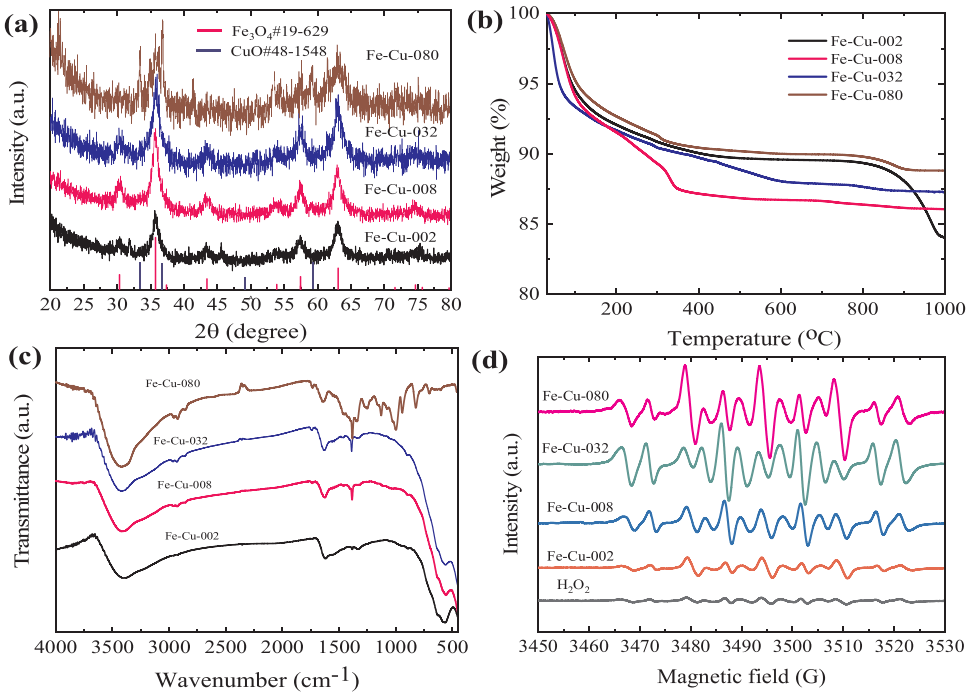

Fig. 2. (a) XRD patterns, (b) TGA curves, (c) FTIR spectra, and (d) EPR spectra of as prepared Fe-Cu-x NPs.

The thermal stability of composites was examined using TGA analysis under nitrogen atmosphere condition. As shown in Fig. 2b, all Fe-Cu-x composites exhibited good thermal stability with negligible mass loss at temperature up to 1000 °C. Weight loss were observed for two phases in Fe-Cu composites. The first phase was adsorbed water between 30 and 300 °C. The second phase, loss occurred at greater than 300 °C, attributed to phase transformation of Fe_3O_4/CuO. The weight loss of Fe-Cu-002, Fe-Cu-008, Fe-Cu-032, and Fe-Cu-080 were about 16, 14, 13, and 12 %, respectively, which indicated that increase in Cu content substantially enhanced the thermal stability of composite due to strong interactions between Fe and Cu oxides.

FTIR was used to characterize the chemical functionality of the Fe-Cu composites. Fig. 2**c** shows the transmittance spectra of the catalyst composites. The appearance of broad band at approximately $3600-330\ cm^{-1}$was due to the stretching vibration of O—H group of adsorbed water [17]. The band at $1632\ cm^{-1}$ was assigned to the bending vibration of water molecules [18]. The band at $554\ cm^{-1}$ was the characteristic stretching vibration of Fe—O within Fe_3O_4 [19]. Three peaks at $1257\ cm^{-1}$, $1126\ cm^{-1}$, and $1010\ cm^{-1}$, corresponding to the stretching vibration of hydroxyl groups of metal oxide were observed in Fe-Cu-080 [20]. In addition, a small peak at $624\ cm^{-1}$ was associated with the Cu—O stretching mode. Results of FTIR analysis clearly demonstrated the formation of Fe and Cu oxides in the composites.

Spin-trapping EPR technique was used to examine the role of Cu in the production of active radicals in the heterogeneous Fenton reaction (Fig. 2d). EPR signals of $OH^{\cdot}$ and $OOH^{\cdot}$ radicals were clearly detected in all five systems. A very weak signal was observed for H_2O_2 without catalyst. Note that many catalysts could activate H_2O_2 to generate reactive radical species to same extent. However, Fe-Cu composited exhibited much stronger signal intensity, which increased with increase in Cu content, suggesting high H_2O_2 activation activity. Fe-Cu-080 displayed the highest signal intensity and H_2O_2 activation capacity among all catalysts studied.

The bimetallic structure of Fe-Cu-080 was further characterized by TEM and HRTEM. The Fe and Cu oxide nanoparticles were round shaped and particle size of 12 ± 6 nm (Fig. 3a). The HRTEM image exhibited lattice fringe spacing of 0.36 nm and 0.25 nm corresponding to the (021) and (311) crystal planes of CuO and Fe_3O_4, respectively (Fig. 3b). The result agreed with that obtained from XRD analysis. Both Fe_3O_4 and CuO had similar particle size and were in tight contact with each other, which may be a favorable situation for charge transfer between Fe_3O_4 and CuO and the activation of H_2O_2. EDS was used to analyze the surface elemental composition of the area in the purple frame of the SEM image (Fig. 3c). EDS results showed that Fe, Cu, and O were major components, being uniformly dispersed on the surface of the composite. The weight ratio of Fe to Cu was close to 16.4:1, which was consistent with the designed amount. Results clearly indicated the full utilization of both metal ions during synthesis.

The distribution of atomic species on the Fe-Cu-080 surface was determined by EPMA. Fig. 4 shows the back scatter images of Fe-Cu-080 together with the elemental mapping for Fe, Cu, and O. Results indicated that the Fe and Cu oxide NPs were remarkably uniform spherical particles highly dispersed over the whole surface of Fe-Cu-080 composite. Results of elemental mapping of composites also showed that Fe and Cu NPs were adjacent to near each other as Janus-type structure, which would increase accessible sites and improve the catalytic reactivity of Fe-Cu bimetallic particle [21]. Furthermore, Cu reduction of Fe^{3+} regenerated Fe^{2+}, which enhanced hydroxyl radicals formation according to the Fenton reaction [8].

3.2. Catalytic performance of bimetallic Fe-Cu composite

The catalytic activity of bimetallic Fe-Cu composites was studied by MB oxidation in heterogenous Fenton process at pH-7. As shown in Fig. 5a, there was no significant removal of MB in 60 min in the presence of H_2O_2 i.e.; a control experiment. MB removal slightly increased to 31 %, 45 %, respectively, upon the addition of CuO, Fe_3O_4. Besides, adsorption experiments were carried without H_2O_2, as to evaluate the extent of MB on catalysts. Results showed that less than 7% of MB were removed by adsorption (**Fig. S1**). Enhanced MB removal occurred over bimetallic Fe-Cu composites when Cu content was increased. Fe-Cu-080 exhibited the highest MB degradation at 99 % in 60 min, which agreed with the highest radical production confirmed by EPR results. Meanwhile, MB removal was 65, 81, and 91 % for Fe-Cu-002, Fe-Cu-008, and Fe-Cu-032, respectively.

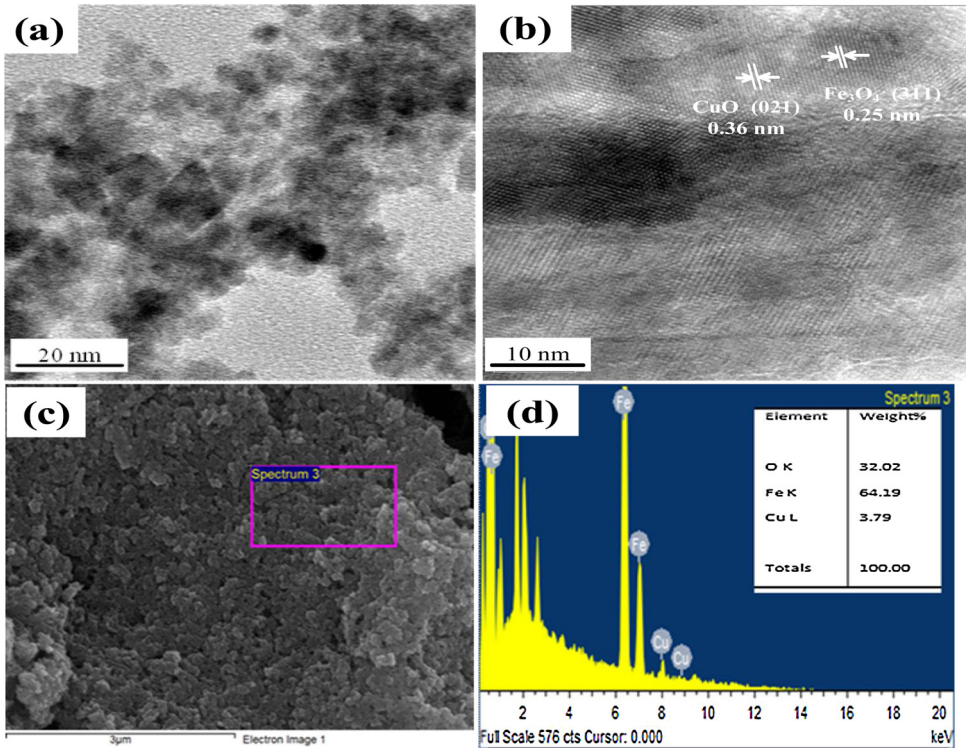

Fig. 3. (a) TEM, (b) HRTEM, (c) SEM, and (d) EDS analysis of as prepared Fe-Cu-x NPs.

The rate of MB degradation followed the pseudo-first-order kinetic model. The observed rate constant k_{obs} (min^{-1}) was determined from the slope of the linear $ln(C_t/C_0)$ vs. treatment time (t) plot, where C_0 and C_t are the MB concentration at the initial (t = 0) and at time t, respectively (Eq. (1)).

$$ln\frac{C_t}{C_0} = -k_{obs}t \quad (1)$$

As shown in Fig. 5b, the pseudo-first-order rate constant, k_{obs}, followed the same trend of the percent MB removal. The k_{obs} values of monometallic catalyst was 6.2×10^{-3} and $1.0 \times 10^{-2}\,min^{-1}$, respectively, for CuO and Fe_3O_4 catalyst (Fig. 5b). Obviously, k_{obs} value

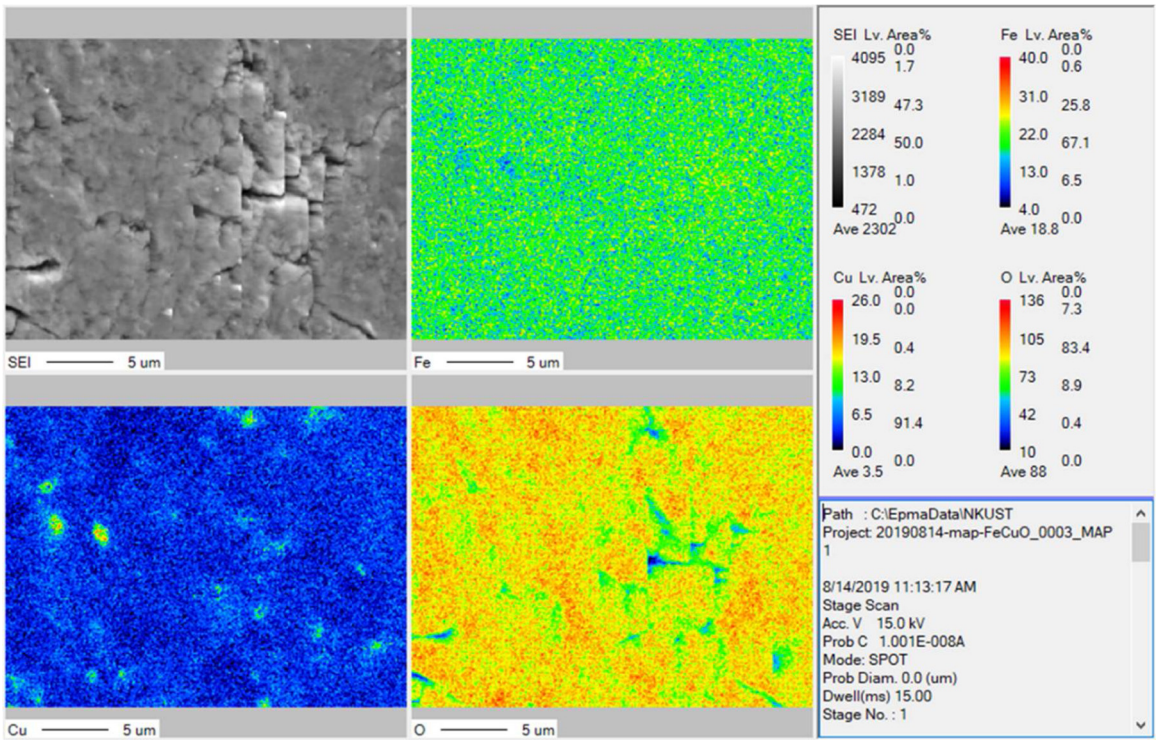

Fig. 4. Backscatter SEM image of Fe-Cu-080 and the related EPMA elemental mapping of Fe, Cu, and O atoms.

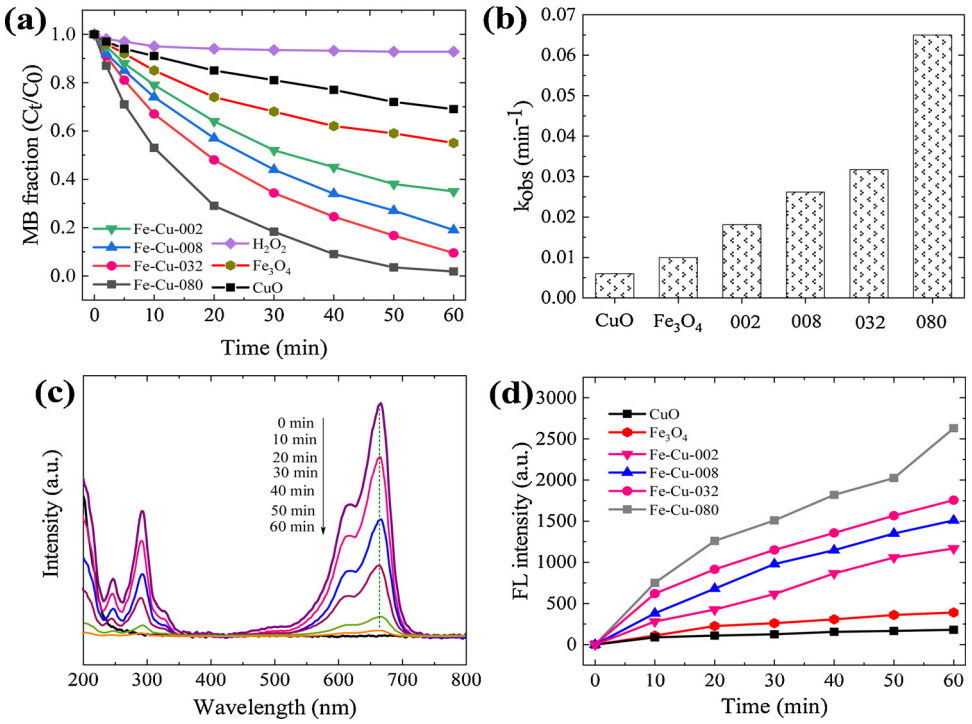

Fig. 5. Effect of different catalysts on activation of H_2O_2 for (a) MB degradation, and (b) k_{obs}. (c) Time-dependent UV–vis absorption spectra of MB, and (d) Time-dependence of the fluorescence intensity at 426 nm.

Table 1
Comparison of degradation of MB by Fenton-like methods by different catalyst.

Catalyst	MB(mg L^{-1})	Catalyst dosage (g L^{-1})	Time (min)	Efficiency (%)	k_{obs} (min^{-1})	Reference
Fe-Cu-080	5	0.5	60	> 99	6.56×10^{-2}	This study
Ferrocene	10	0.372	120	> 99	6.17×10^{-3}	[22]
Fe_3O_4/rGO	10	0.3	120	98.6	2.6×10^{-3}	[23]
Reduced $CuFe_2O_4$	50	0.1	25	> 70	5.5×10^{-2}	[24]
$Fe_3O_4/SiO_2/C$	50	1	140	82	3.6×10^{-2}	[25]
Fe_3O_4/CeO_2	100	1	120	> 99	2×10^{-2}	[26]
Fe_3O_4/galic acid/GO	64	1	200	> 99	1.2×10^{-2}	[27]
N,C/CuO-Fe_2O_3	75	0.1	180	97.4	1.08×10^{-2}	[28]
FeNi/C-300	30	1	60	> 80	1.05×10^{-2}	[29]
$Ba_{0.4}Sr_{0.6}Al_{0.4-x}Sm_xFe_{11.60}O_1$	10	0.25	140	> 99	6.51×10^{-2}	[30]

increased remarkably from 1.81×10^{-2} to 6.56×10^{-2} min^{-1} with increase in Cu mass loading from 0.02 mmol (Fe-Cu-002) to 0.8 mmol (Fe-Cu-080), respectively. The difference in MB removal efficiency between monometallic and bimetallic catalysts strongly suggested a synergistic effect between Fe and Cu via redox reaction, which ensured constant supply of metal ions, namely, Fe^{2+}, for H_2O_2 decomposition, hydroxyl radicals production, and MB oxidation [8]. Results also indicated that the catalytic activity of bimetallic Fe-Cu composite in Fenton-like reaction was highly dependent on the Fe-Cu ratio. For example, Fe-Cu-080 had smaller particle size and high efficiency in radical production, which gave the best catalytic activity among all Fe-Cu composites studied. Furthermore, Table 1 showed the k_{obs} value for MB degradation by different Fenton-like catalysts. Results indicated that Fe-Cu-080 exhibited k_{obs} greater than or comparable to most reported data [22–30]; Fe-Cu-080 catalyst, indeed, was a promising Fenton-like catalyst.

Fig. 5c shows the temporal change of UV–vis spectra in the range of 200 − 800 nm of aqueous MB solution in the presence H_2O_2 and Fe-Cu-080 catalyst. Two main absorbance peaks were observed. The peak at 292 nm was ascribed to the π → π* transition related to unsaturated conjugate aromatic rings [31]. The absorption peak at 664 nm was attributed to the chromophores functional groups of MB and its dimers, namely −C═S and −C═N, which might undergo hemolytic cleavage [32]. Note that both absorption peaks at 292 and 664 nm rapidly decreased with reaction time and almost disappeared at the end of 60 min. The rapid attenuation of peak at 664 nm, indicated the breakup of the characteristic color of the conjugate structure in MB molecule. The disappearance of absorbance at 292 nm was attributed to the degradation of aromatic fragments of MB and its intermediates.

In order to establish the relationship between the concentration and the hydroxyl radical availability during the reaction time, the concentration $OH^{\cdot}$ radicals were determined by the terephthalic acid fluorescence (FL) probe method [33]. The photoluminescence spectrum of 2-hydroxyterephthalic acid production from the reaction between $OH^{\cdot}$ and terephthalic acid (**Eq. 2**) was recorded at 426 nm, using 312 nm as the excitation wavelength (**Fig. S2**). The $OH^{\cdot}$ radical generation in correlation with fluorescence intensity as a function of H_2O_2 activation time by different catalysts is plotted in Fig. 5**d**. It was observed that more $OH^{\cdot}$ was generated in the presence of Fe-Cu-080 composite, which coincided with the trend of MB degradation. Since Fe-Cu-080 exhibited the best catalytic activity in comparison with other catalysts including monometallic catalyst, it was used for further studies.

The influence of initial pH on MB degradation performance of Fe-

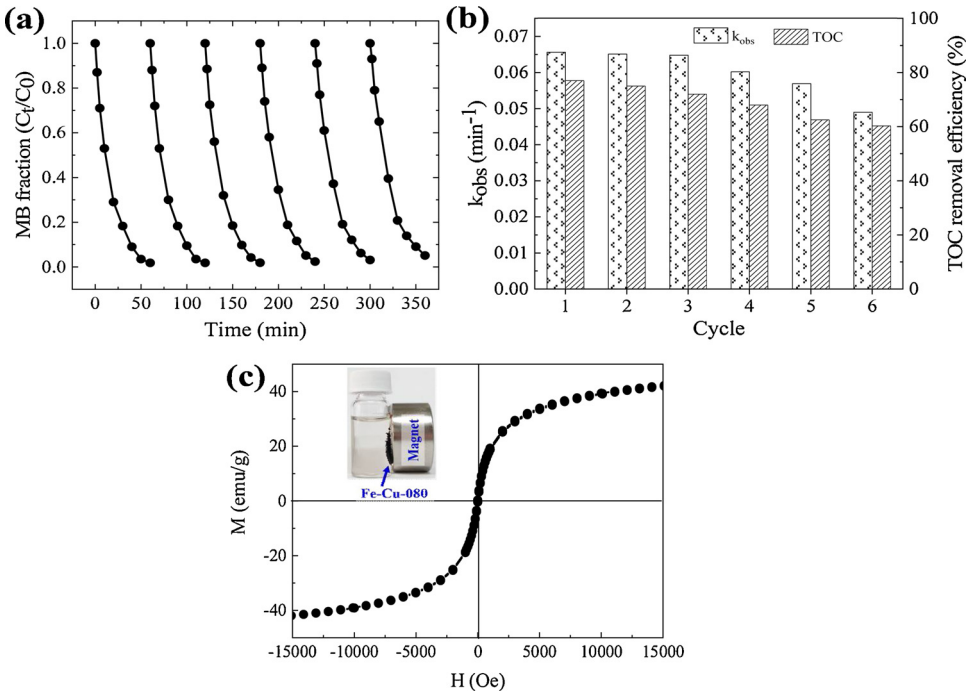

Fig. 6. Recyclability experiments on activation of H_2O_2 by Fe-Cu-080 for (a) MB degradation, and (b) TOC removal. (c) Magnetic hysteresis loops of Fe-Cu-080 catalyst (Inset shows their suspension after magnetic separation by an external magnet).

Cu-080/H_2O_2 system was carried out at different pH value from 3 to 11 (**Fig. S3a**). It was observed that the degradation efficiencies were more than 90 % and satisfactory in a wide pH range. The degradation efficiency of MB at alkaline condition was slightly lower than that of acidic and neutral conditions due to the instability of H_2O_2 in an alkaline solution. Therefore, Fe-Cu-080/H_2O_2 system could work in a wide range pH, which obviously overcame the drawback of conventional Fenton oxidation process that required acidic pH. Moreover, leaching study for the as-prepared Fe-Cu-080 catalyst at different pHs after 60 min of reaction was also carried out to investigate its stability. As shown in **Fig. S3b**, the Fe-Cu-080 showed the good stability in Fenton-like process at different pHs., especially for that the total metal leaching observed at pH-3 only accounted for 0.23 % of the total metal content at applied catalyst dosage of 0.5 g L^{-1}.

3.3. Recyclability of bimetallic Fe-Cu composite and degradation of MB in natural water samples

The stability and reusability of catalyst is vitally important to engineering applications. Fig. 6**a** displays the results of MB degradation by H_2O_2 in the presence of Fe-Cu-080 catalyst in six consecutive runs under same experimental condition as mentioned above. It was clearly observed that the MB removal percentage remained nearly constant at around 95 % for all six runs. The observed rate constant remained unchanged during the first 3 cycles at 6.5 × 10^{-2} min^{-1}, and slightly decreased to 6.4 × 10^{-2} min^{-1} at the forth, 5.7 × 10^{-2} min^{-1} at the 5th cycle, and 4.9 × 10^{-2} min^{-1} at the 6th cycle (Fig. 6b). Meanwhile, the slight decrease in mineralization from 77 % for the 1st cycle to 60.3 % for the 6th cycle, also indicated relatively stable catalytic potential in repeated cycles. Obviously, the leaching of metal species was accompanied with loss of active sites [17]. Furthermore, adsorption of intermediates and residual MB onto the active sites of Fe-Cu-080, hindered the interaction between Fe-Cu-080 NPs and H_2O_2 molecules [34]. Fig. 6**c** shows the magnetic hysteresis loop of Fe-Cu-080 measured at room temperature. The saturation magnetization was 41.2 emu g^{-1} for Fe-Cu-080, which enabled significant magnetic response to magnetic field for the separation of spent catalysts (inset of Fig. 6c). All results confirmed the stability, reusability, and facile magnetic separation of developed Fe-Cu composite.

From an applicative standpoint, the composition of actual wastewater is extremely complex. Therefore, the degradation of MB requires to be measured in a real matrix to assess the differences between simulated wastewater and actual polluted wastewater. In this work, the removal efficiency of MB by Fe-Cu-080/H_2O_2 system was studied in ultrapure water, tap water (Center for the study of sediment, Kaohsiung City, Taiwan), river water (Chengcing lake, Kaohsiung City, Taiwan), and municipal wastewater (sewage treatment plant, National Kaohsiung University of Science and Technology, Kaohsiung City, Taiwan). The collected water samples were spiked with 5 mg L^{-1} MB, adjusting the pH at 7. According to **Fig. S4**, more than 95 % of MB was removed by Fe-Cu-080/H_2O_2 system for ultrapure water, tap water and lake water. While the composition of wastewater had a slight negative influence on the removal of MB, leading to a relatively lower removal of MB (~ 93 %). The obtained results greatly indicated that the composition of real wastewater did not impede the activity of Fe-Cu-080/H_2O_2 system, thereby proving the effectiveness of Fe-Cu bimetallic catalyst in Fenton-like process for real wastewater treatment.

3.4. Toxicity evaluation of Fe-Cu composite

A series of cell viability studies were performed using NRK-52E cells treated by Fe-Cu-080 NPs, Fe_3O_4 NPs, and CuO NPs with different particle concentrations (0, 25, 50, 100, 250, and 500 μg mL^{-1}). The result (**Fig. S5**) shows that the survival rate of NRK-52E cells treated by CuO NPs at the higher concentration (500 μg mL^{-1}) was only 8 %, which indicated that CuO NPs seriously damaged the cells; and was consistent with our previous study [35]. In contrast, NRK-52E cells, treated by Fe_3O_4 NPs of high dose (500 μg mL^{-1}) did not cause cell death and the cell survival rate was 100 %. Moreover, the viability of NRK-52E cells treated by Fe-Cu-080 NPs was still above 94 %. Results clearly showed that the Fe-Cu-080 was not cytotoxic and could greatly reduce the copper toxicity.

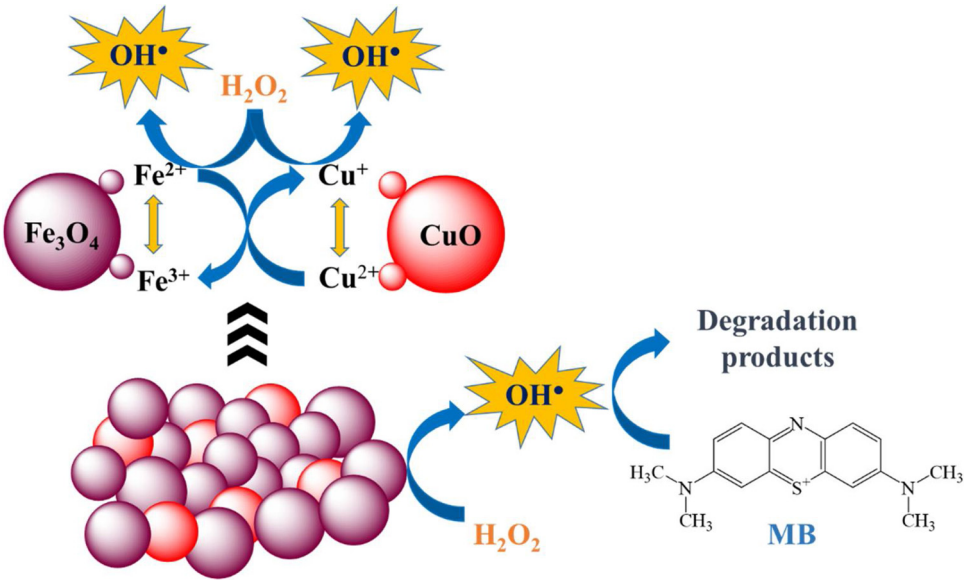

Fig. 7. Schematic diagram of the reaction mechanism of the H_2O_2 activation by Fe-Cu-080 catalyst.

3.5. Reaction mechanism in the Fe-Cu bimetallic system

Based on the results obtained above, a preliminary reaction mechanism on the catalytic degradation of MB by H_2O_2 over Fe-Cu bimetallic composite was proposed (Fig. 7). The heterogeneous Fenton reaction catalyzed by Fe-Cu-080 proceeds via surface reaction involving both Fe_3O_4 and CuO active sites. Specifically, Fe^{2+} and Cu^{+} can catalyze H_2O_2 decomposition to produce $OH^{\cdot}$ radicals, and then the regeneration of Fe^{2+} and Cu^{+} by the reduction reaction with H_2O_2 (Eqs. (3)–(6)) [36,37]. In addition, the reduction of Fe^{3+} by Cu^{+} was spontaneous according to the standard reduction potentials of the Fe and Cu (Eqs. (7) and (8)), which benefited the continuous redox cycles of Fe^{3+}/Fe^{2+} and Cu^{+}/Cu^{2+} pair in Fe-Cu-080/H_2O_2 system (Eq. 9). Consequently, more H_2O_2 would react with the active sites via Fenton process and result in production of higher $OH^{\cdot}$ radicals as shown in the following equations.

$$\equiv Fe^{2+} + H_2O_2 \rightarrow \equiv Fe^{3+} + OH^{\cdot} + OH^{-} \quad (3)$$

$$\equiv Fe^{3+} + H_2O_2 \rightarrow \equiv Fe^{2+} + HO_2^{\cdot} + H^{+} \quad (4)$$

$$\equiv Cu^{+} + H_2O_2 \rightarrow \equiv Cu^{2+} + OH^{\cdot} + OH^{-} \quad (5)$$

$$\equiv Cu^{2+} + H_2O_2 \rightarrow \equiv Cu^{+} + HO_2^{\cdot} + H^{+} \quad (6)$$

$$\equiv Fe^{3+} + e^{-} \rightarrow \equiv Fe^{2+} E_0 = 0.77\,V \quad (7)$$

$$\equiv Cu^{2+} + e^{-} \rightarrow \equiv Cu^{+} E_0 = 0.17\,V \quad (8)$$

$$\equiv Fe^{3+} + Cu^{+} \rightarrow \equiv Fe^{2+} + \equiv Cu^{2+} \Delta E_0 = 0.6\,V \quad (9)$$

3.6. Degradation pathway of MB

HPLC/MS/MS was used to identify the intermediates during the reaction and to establish the pathway of MB degradation in the Fe-Cu-080/H_2O_2 system. **Fig. S6a** showed a high intense single peak of at m/z = 284 ascribed to the parent MB molecule. After 60 min, no MB was observed and the occurrence of new peaks attributed to the production of intermediates shown in **Fig. S6b**. Based on the intermediate products identified, a possible degradation pathway of MB by the Fe-Cu-080/H_2O_2 system is proposed primarily, as given in Fig. 8. Initially, the $OH^{\cdot}$ preferentially hydroxylated the methyl group connected with nitrogen atoms on the side ring and the C–S^{+}–C at the center, leading to the formation of fragments corresponding to m/z = 325. Then the sulfone was formed in MB molecules corresponding to the observed fragment at m/z = 264. Finally, the disruption of the two side aromatic rings took place and the resultant smaller intermediates subsequently undergo successive degradation reactions to yield carbon dioxide and water, resulting in a decrease in TOC concentration. Thus, HPLC-MS/MS results strongly confirm catalytic degradation and mineralization of MB dye by $^{\cdot}OH$ produced by the catalyst.

4. Conclusion

A magnetic Fe-Cu bimetallic composite was synthesized via a facile precipitation method. The as-synthesized Fe-Cu bimetallic composites with different Cu mass loadings were characterized by a series of surface analysis techniques. The Fe-Cu-080 composite with appropriate amount of Cu could effectively controled the size of bimetallic particles to enable uniform distribution in the nano-sized range, and facilitated the catalytic activity in heterogeneous Fenton reaction with 99 % removal of MB within 60 min. EPR and FL results proved that the $OH^{\cdot}$ radical generated in Fe-Cu composite/H_2O_2 system was involved in the degradation of MB. Fe-Cu-080 was stable and reusable at least for six consecutive cycles. The magnetic nature of Fe-Cu-080 composite enabled its easy separation from aqueous solution in simple external magnetic field. Exhibited low cellular toxicity and magnetic properties, which renders the catalyst promising for the treatment of organic wastewater. Furthermore, our findings may expand further development of other Fe-Cu bimetallic catalysts for degradation of organic pollutants by Fenton-like process.

CRediT authorship contribution statement

Thanh Binh Nguyen: Conceptualization, Methodology, Writing - original draft. **Cheng-Di Dong:** Data curation, Validation. **C.P. Huang:** Writing - review & editing. **Chiu-Wen Chen:** Resources. **Shu-Ling Hsieh:** Resources. **Shuchen Hsieh:** Supervision.

Declaration of Competing Interest

The authors declare that they have no known competing financial interests or personal relationships that could have appeared to influence the work reported in this paper.

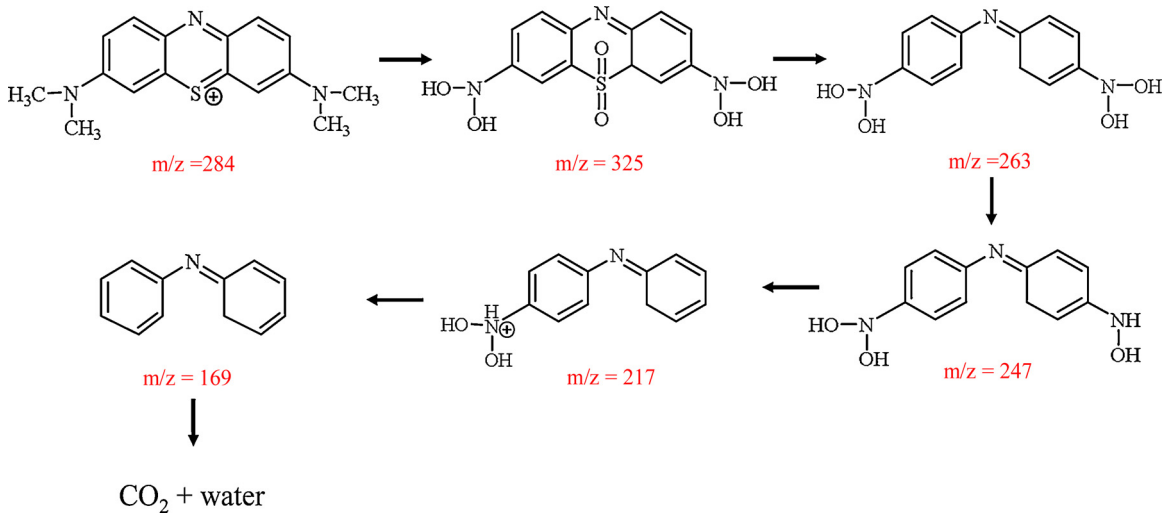

Fig. 8. Proposed degradation pathway of MB by Fe-Cu-080/H_2O_2 system.

Acknowledgments

The authors wish to thank the Ministry of Science and Technology (MOST), Taiwan, for generous financial support under grant No. 106-2221-E-002-002-MY3 and 108-2113-M-110-004. Addition support was provided by US NSF IOA (1632899) to CPH.

Appendix A. Supplementary data

Supplementary material related to this article can be found, in the online version, at doi:https://doi.org/10.1016/j.jece.2020.104139.

References

[1] T. Sruthi, R. Gandhimathi, S.T. Ramesh, P.V. Nidheesh, Stabilized landfill leachate treatment using heterogeneous Fenton and electro-Fenton processes, Chemosphere 210 (2018) 38–43.
[2] A.I. Zarate-Guzman, L.V. Gonzalez-Gutierrez, L.A. Godinez, A. Medel-Reyes, F. Carrasco-Marin, L.A. Romero-Cano, Towards understanding of heterogeneous Fenton reaction using carbon-Fe catalysts coupled to in-situ H_2O_2 electro-generation as clean technology for wastewater treatment, Chemosphere 224 (2019) 698–706.
[3] S.C. Hsieh, P.Y. Lin, FePt nanoparticles as heterogeneous Fenton-like catalysts for hydrogene peroxide decomposition and the decolorization of methylene blue, J. Nanopart. Res. 14 (2012) 956.
[4] S. Navalon, M. Alvaro, H. Garcia, Heterogeneous Fenton catalysts based on clays, silicas and zeolites, Appl, Catal. B Environ. 99 (2010) 1–26.
[5] M. Munoz, Z.M. de Pedro, J.A. Casas, J.J. Rodriguez, Preparation of magnetite-based catalysts and their application in heterogeneous Fenton oxidation - A review, Appl. Catal. B-Environ. 176 (2015) 249–265.
[6] C.D. Dong, C.W. Chen, C.M. Kao, C.C. Chien, C.M. Hung, Wood-biochar-supported magnetite nanoparticles for remediation of PAH-Contaminated estuary sediment, Catalysts 8 (2018) 13.
[7] C.D. Dong, M.L. Tsai, C.W. Chen, C.M. Hung, Heterogeneous persulfate persulfate oxidation of BTEX and MTBE using Fe_3O_4-CB magnetite composites and the cytotoxicity of degradation products, Int. Biodeter. Biodegr. 124 (2017) 109–118.
[8] K.Y. Li, Y.Q. Zhao, M.J. Janik, C.S. Song, X.W. Guo, Facile preparation of magnetic mesoporous Fe_3O_4/C/Cu composites as high performance Fenton-like catalysts, Appl. Surf. Sci. 396 (2017) 1383–1392.
[9] M.M.H. Guerra, I.O. Alberola, S.M. Rodriguez, A.A. Lopez, A.A. Merino, A.E.C. Lopera, J.M.Q. Alonso, Oxidation mechanisms of amoxicillin and paracetamol in the photo-Fenton solar process, Water Res. 156 (2019) 232–240.
[10] Z. Eren, N.H. Ince, Sonolytic and sonocatalytic degradation of azo dyes by low and high frequency ultrasound, J. Hazard. Mater. 177 (2010) 1019–1024.
[11] A.L. Garcia-Costa, J.A. Zazo, J.A. Casas, Microwave-assisted catalytic wet peroxide oxidation: energy optimization, Sep. Purif. Technol. 215 (2019) 62–69.
[12] A.N. Pham, G.W. Xing, C.J. Miller, T.D. Waite, Fenton-like copper redox chemistry revisited: hydrogen peroxide and superoxide mediation of copper-catalyzed oxidant production, J. Catal. 301 (2013) 54–64.
[13] Sun Y, Z. Yang, P. Tian, Y. Sheng, J. Xu, Y.F. Han, Oxidative degradation of nitrobenzene by a Fenton-like reaction with Fe-Cu bimetallic catalysts, Appl. Catal. B Environ. 244 (2019) 1–10.
[14] F. Denizot, R. Lang, Rapid colorimetric assay for cell growth and survival: modification to the tetrazolium dye procedure giving improved sensitivity and reliability, J. Immunol. Methods 89 (1986) 271–277.
[15] B. Lai, Y.H. Zhang, Z.Y. Chen, P. Yang, Y.X. Zhou, J.L. Wang, Removal of p-nitrophenol (PNP) in aqueous solution by the micron-scale iron-copper (Fe/Cu) bimetallic particles, Appl. Catal. B Environ. 144 (2014) 816–830.
[16] R.S. Sahu, Y.H. Shih, Reductive debromination of tetrabromobisphenol A by tailored carbon nitride Fe/Cu nanocomposites under an oxic condition, Chem. Eng. J. 378 (2019) 9.
[17] T.B. Nguyen, R.A. Doong, C.P. Huang, C.W. Chen, C.D. Dong, Activation of persulfate by CoO nanoparticles loaded on 3D mesoporous carbon nitride (CoO@meso-CN) for the degradation of methylene blue (MB), Sci. Total Environ. 675 (2019) 531–541.
[18] S. Goldberg, Competitive adsorption of arsenate and arsenite on oxides and clay minerals, Soil Sci. Soc. Am. J. 66 (2002) 413–421.
[19] N.M. Mahmoodi, Z. Hosseinabadi-Farahani, F. Bagherpour, M.R. Khoshrou, H. Chamani, F. Forouzeshfar, Synthesis of CuO-NiO nanocomposite and dye adsorption modeling using artificial neural network, Desalin. Water Treat. 57 (2016) 17220–17229.
[20] T. Liu, K. Wu, W. Xue, C. Ma, Characteristics and mechanisms of arsenate adsorption onto manganese oxide-doped aluminum oxide, Environ. Prog. Sustain. Energy 34 (2015) 1009–1018.
[21] J. Trujillo-Reyes, V. Sanchez-Mendieta, A. Colin-Cruz, R.A. Morales-Luckie, Removal of indigo blue in aqueous solution using Fe/Cu nanoparticles and C/Fe-Cu nanoalloy composites, Water Air Soil Pollut. 207 (2010) 307–317.
[22] Q. Wang, S. Tian, P. Ning, Degradation mechanism of methylene blue in a heterogeneous Fenton-like reaction catalyzed by a ferrocene, Ind. Eng. Chem. Res. 53 (2014) 543–649.
[23] W. Liu, J. Qian, K. Wang, H. Xu, D. Jiang, Q. Liu, X. Yang, H. Li, Magnetically separable Fe3O4 nanoparticle-decorated reduced graphene oxide nanocomposite for catalytic wet hydrogen peroxide oxidation, J. Inorg. Organome. Polym. Mater 23 (2013) 907–916.
[24] Q. Qin, Y. Liu, X. Li, T. Sun, Y. Xu, Enhanced heterogeneous Fenton-like degradation of methylene blue by reduced $CuFe_2O_4$, RSC Adv. 8 (2018) 1071–1077.
[25] X. Liu, Q. Zhang, B. Yu, R. Wu, J. Mai, R. Wang, L. Chen, S.T. Yang, Preparation of Fe_3O_4/TiO_2/C nanocomposites and their application in Fenton-like catalysis for dye decoloration, Catalysts 6 (2016) 146.
[26] K. Li, Y. Zhao, C. Song, X. Guo, Magnetic ordered mesoporous Fe_3O_4/CeO_2 composites with synergy of adsorption and Fenton catalysis, Appl. Surf. Sci. 425 (2017) 526–534.
[27] Y. Hua, S. Wang, J. Xiao, C. Cui, C. Wang, Preparation and characterization of Fe_3O_4/galic acid/graphene oxide magnetic nanocomposites as highly efficient Fenton catalysts, RSC Adv. 46 (2017) 28979–28986.
[28] B. Ren, J. Miao, Y. Xu, Z. Zhai, X. Dong, S. Wang, L. Zhang, Z. Liu, A grape-like N-doped carbon/CuO-Fe_2O_3 nanocomposite as a highly active heterogeneous Fenton-like catalyst in methylene blue degradation, J. Clean. Prod. 240 (2019) 118143.
[29] D. Li, T. Yang, Y. Li, Z. Liu, W. Jiao, Facile and green synthesis of highly dispersed tar-based heterogeneous Fenton catalytic nanoparticles for the degradation of methylene blue, J. Clean. Prod. 246 (2020) 119033.
[30] G.A. Ashraf, R.T. Rasool, M. Hassan, L. Zhang, Enhanced photo Fenton-like activity by effective and stable Al–Sm M-hexaferrite heterogenous catalyst magnetically detachable for methylene blue degradation, J. Alloys. Compd. 821 (2020) 153410.
[31] C.M. Hung, C.W. Chen, Y.Y. Liu, C.D. Dong, Decolorization of methylene blue by persulfate activated with FeO magnetic particles, Water Environ. Res. 88 (2016) 675–686.
[32] L.G. Devi, B.N. Murthy, S.G. Kumar, Heterogeneous photo catalytic degradation of anionic and cationic dyes over TiO_2 and TiO_2 doped with Mo^{6+} ions under solar light: correlation of dye structure and its adsorptive tendency on the degradation rate, Chemosphere 76 (2009) 1163–1166.
[33] T. Hirakawa, Y. Nosaka, Properties of O-2(center dot-) and OH center dot formed in

TiO_2 aqueous suspensions by photocatalytic reaction and the influence of H_2O_2 and some ions, Langmuir 18 (2002) 3247–3254.
[34] V.T. Nguyen, T.B. Nguyen, C.W. Chen, C.M. Hung, C.P. Huang, C.D. Dong, Cobalt-impregnated biochar (Co-SCG) for heterogeneous activation of peroxymonosulfate for removal of tetracycline in water, Bioresour. Technol. Rep. 292 (2019) 8.
[35] M.L. Kung, S.L. Hsieh, C.C. Wu, T.H. Chu, Y.C. Lin, B.W. Yeh, S.C. Hsieh, Enhanced reactive oxygen species overexpression by CuO nanoparticles in poorly differentiated hepatocellular carcinoma cells, Nanoscale 7 (2015) 1820–1829.
[36] Q.C. Do, D.G. Kim, S.O. Ko, Nonsacrificial template synthesis of magnetic-based yolk-shell nanostructures for the removal of acetaminophen in Fenton-like systems, ACS Appl. Mater. Interfaces 9 (2017) 28508–28518.
[37] P.V. Nidheesh, Heterogeneous Fenton catalysts for the abatement of organic pollutants from aqueous solution: a review, RSC Adv. 5 (2015) 40552–40577.